# Detection of Hepatitis B Virus DNA with a Paper Electrochemical Sensor

Xiang Li, Karen Scida, and Richard M. Crooks*

Department of Chemistry, The University of Texas at Austin, 105 East 24th Street, Stop A5300, Austin, Texas 78712-1224, United States

Ⓢ Supporting Information

ABSTRACT: Here we show that a simple paper-based electrochemical sensor, fabricated by paper folding, is able to detect a 30-base nucleotide sequence characteristic of DNA from the hepatitis B virus (HBV) with a detection limit of 85 pM. This device is based on design principles we have reported previously for detecting proteins via a metalloimmunoassay. It has four desirable attributes. First, its design combines simple origami (paper folding) assembly, the open structure of a hollow-channel paper analytical device to accommodate micrometer-scale particles, and a convenient slip layer for timing incubation steps. Second, two stages of amplification are achieved: silver nanoparticle labels provide a maximum amplification factor of 250 000 and magnetic microbeads, which are mobile solid-phase supports for the capture probes, are concentrated at a detection electrode and provide an additional ∼25-fold amplification. Third, there are no enzymes or antibodies used in the assay, thereby increasing its speed, stability, and robustness. Fourth, only a single sample incubation step is required before detection is initiated.
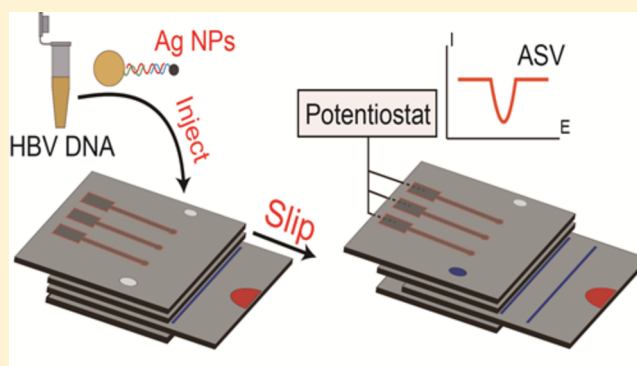
In this article we show that a simple paper-based electrochemical sensor, fabricated by paper folding, is able to detect DNA from the hepatitis B virus (HBV) with a detection limit of 85 pM. This device, which we call oSlip-DNA (o stands for origami,[1] Slip indicates that it incorporates a slip layer,[2,3] and DNA means that it is configured for DNA detection),[4] is based on design principles reported previously for detecting proteins via a metalloimmunoassay.[4,5] The oSlip-DNA has four desirable attributes. First, its design combines a simple origami (paper folding) assembly,[1] the open structure of a hollow-channel paper analytical device to accommodate micrometer-scale particles,[6] and a convenient component (the slip layer) for timing incubation steps.[3,7] Second, two stages of amplification are achieved in the oSlip-DNA: (1) silver nanoparticle labels (AgNPs, 20 nm diameter, ∼250 000 atoms per AgNP) provide a maximum amplification factor of 250 000 and (2) magnetic microbeads (MμBs), which are mobile solid-phase supports for the capture probes, are concentrated at a detection electrode and lead to an additional ∼25-fold amplification. Third, there are no enzymes or antibodies used in the assay, thereby increasing speed, stability, and robustness. Fourth, only a single sample incubation step is required before detection is initiated, thereby simplifying sample preparation. Here, we illustrate these basic concepts by demonstrating detection of a 30-base nucleotide sequence characteristic of HBV.[8]

HBV infection is one of the most important chronic virus infections with more than 350 million people infected worldwide.[9] It can result in many clinical problems, including liver cirrhosis and hepatocellular carcinoma.[10,11] The DNA from HBV, which is an important biomarker for HBV infection, can vary from a few to more than 10^9 copies/mL in serum, and it is usually detected in serum[12] or dried blood spots[13] by tests based on polymerase chain reaction (PCR).[14,15] These PCR assays are usually performed in centralized laboratory settings due to the specialized nature of the required equipment and personnel.[16] More recently, several types of biosensors have been developed to detect the HBV DNA, including patterned nanoarrays with surface-enhanced Raman scattering detection[17] and a gold nanorod-based fluorescence resonance energy transfer system.[18] However, these sensors suffer from either a long testing time (>30 min) or high cost, which makes them less than ideal for point-of-care (POC) applications. The device we report here is intended to fill the need for a cheaper, more portable detection system.

Paper-based analytical devices (PADs) for POC applications were popularized as early as the mid-1960s.[19] For example, one of the most familiar applications of PADs that emerged from these early studies is the pregnancy test strip, which is based on a lateral flow immunoassay.[20] In the mid-2000s, the Whitesides group disrupted the lateral flow assay technology by introducing 2D and 3D PADs.[21−23] These were fabricated on

filter paper using photoresist[21,24] or wax[25] to create fluidic channels. Capillary flow in such sensors is driven by the cellulose matrix,[26] and therefore no pump or external power supply is required. The low cost and ease of remediating filter paper makes it a good candidate for POC applications.[23,27,28] Finally, a number of detection methods, including colorimetry,[29,30] electrochemistry,[4,31−33] UV−vis,[34] Raman,[35,36] fluorescence,[37,38] electrochemiluminescence,[39,40] and mass spectrometry[41] have been successfully applied to PAD assays. Of these detection methods, electrochemical methods are perhaps the most useful,[42,43] because they are quantitative, lend themselves to miniaturization, have low power requirements, and require only simple detection instrumentation. Accordingly, we have focused on electrochemical detection in our sensor technologies.

Microbeads, particularly those having a magnetic core, are a mainstay of bioassay systems for three reasons. First, they generally have much higher total surface areas than macroscopic planar surfaces, and therefore they can support more receptors. Second, their mobility in solution decreases assay times by increasing the likelihood of encounters between targets and receptors. Third, washing steps are faster and easier because the beads can be separated from solution by a magnetic force. For these reasons, it seems natural that microbeads would be integrated into PADs as mobile solid-phase supports. However, there is a size incompatibility: the limited pore size of the cellulose matrix is poorly matched with the unhindered flow of micrometer-scale microbeads. We recently resolved this problem by introducing hollow-channel PADs,[6,44,45] in which the cellulose channel is physically removed. Because the thickness of the paper we use is about 180 μm, this leads to an unhindered flow of microbeads.

Another key step in bioassays is precise timing of incubation and washing steps. For PADs, a number of strategies have been introduced for enabling these operations. These include dissolvable barriers,[46] magnetic valves,[47] programmed disconnection,[48] and sequential reagent loading using multiple pathways.[49] We contributed to this functionality by introducing the SlipPAD, which is a device that incorporates a moveable piece of paper that can be used to initiate on-chip chemical reactions at defined times.[2,3] The SlipPAD is simply a paper version of the SlipChip concept first reported by the Ismagilov group.[2,7]

In the present article we combine hollow channels, the SlipPAD methodology, and electrochemical detection to provide a one-step, full sandwich, quantitative DNA assay for HBV. The limit of detection (LOD) is 85 pM, which is too high for early detection of HBV in the absence of DNA amplification. Nevertheless, this is a very good LOD for a user-friendly device costing just $0.36 U.S. dollars (including reagents). Moreover, the performance metrics (LOD, time-to-answer, and linear range) of the oSlip-DNA compare favorably with the same assay carried out in a conventional electrochemical cell. Importantly, the results reported here also demonstrate the ease with which the oSlip platform can be reconfigured. That is, our recently reported biotin/streptavidin assay[4] is converted into an oligonucleotide assay simply by changing the receptor and label recognition elements.

■ EXPERIMENTAL SECTION

Chemicals and Materials. 1× Phosphate buffered saline (PBS) solution (containing 10.0 mM phosphate, 138.0 mM NaCl, and 2.7 mM KCl, pH 7.4) and $KMnO_4$ were purchased from Sigma-Aldrich (St. Louis, MO). Label DNA (5′ thiol-modified C6-S-S-A_{10}-TACCACATCATCCAT 3′), the HBV DNA target (3′ ATG GTG TAG TAG GTA TAT TGA CTT TCG GTT 5′), and capture DNA (5′ ATAACTGAAAGC-CAA-A_{10}-Biotin 3′) were from Integrated DNA Technologies (Coralville, IA) and purified by HPLC. HCl, sodium citrate dihydrate, 4-(2-hydroxyethyl)-1-piperazineethanesulfonic acid (HEPES), NaOH, and Whatman grade 1 chromatography paper (180 μm thick) were obtained from Fisher Scientific (Walthman, MA). AgNPs (20 nm diameter) were from Ted Pella (Redding, CA). Streptavidin-coated MμBs (2.8 μm diameter) were from Bangs Laboratories (Fishers, IN). Erioglaucine disodium salt was acquired from Acros Organics (Pittsburgh, PA). Carbon ink for the screen-printed electrodes (SPEs) was from Engineered Conductive Materials (Delaware, OH). The neodymium cylindrical magnet (N48, 1/16 in. × 1/2 in.) was purchased from Apex Magnets (Petersburg, WV). All solutions were prepared using deionized water (DI, > 18.0 MΩ cm) purified by a Milli-Q Gradient System (Bedford, MA).

Device Fabrication. The oSlip fabrication method has been reported previously, and to demonstrate its ease of reconfigurability we used the same approach for the oSlip-DNA.[4] Briefly, as shown in the Supporting Information (Figures S1 and S2), the oSlip-DNA device pattern was designed in CorelDRAW software and printed on Whatman grade 1 chromatography paper using a wax printer (Xerox ColorQube 8570DN). The patterned paper sheet was placed in an oven at 120 °C for 45 s to melt the wax so that it penetrated through the thickness of the paper. After cooling to 25 ± 2 °C, the hollow channel was cut into the paper using a razor blade. The three electrodes were then added by stencil printing.[33] A binder clip with copper tape on it (Figure S2) was used to connect the screen-printed electrodes to a potentiostat. Before use, 1.0 μL of 1.0 mM erioglaucine solution was drop-cast onto the outlet on the second layer of the device. As discussed later, this makes it possible to know when flow through the channel stops. Finally, the oSlip-DNA was sandwiched between two acrylic plates (Evonik Industries) and secured with binder clips to reproducibly compress the device and ensure uniform thickness of the hollow channel.

Modification of AgNPs and MμBs with DNA. AgNPs modified with label DNA were synthesized using a fast pH-assisted functionalization method first reported by Liu and co-workers.[50,51] A 500.0 μL stock solution of AgNPs (565.0 pM in DI H_2O) was mixed with thiolated DNA at a molar ratio of 1:1000. The mixture was placed on a vortexer for 5.0 min. Next, 26.5 μL of 100.0 mM pH 3.0 citrate-HCl buffer was added to the solution to bring the salt concentration up to 5.0 mM. The solution was vortexed for an additional 5.0 min before adding another 27.8 μL of citrate-HCl buffer to reach a final salt concentration of 10.0 mM. After 25.0 min, 500.0 μL of 100.0 mM pH 7.6 HEPES buffer was added to bring the solution pH back to neutral. The label DNA-modified AgNPs were then centrifuged (20.0 min at 16 000g) and washed three times with 1× PBS buffer (pH 7.4) to obtain the final product. The resulting AgNPs were characterized by UV−vis spectroscopy (Hewlett-Packard HP 8453 spectrometer), zeta potential measurements (Nanosight NS500), and transmission electron microscopy (JEOL 2010F TEM).

Capture DNA immobilization on MμBs takes advantage of biotin/streptavidin conjugation. Briefly, surfactant was removed from a stock solution containing 1.1 pM streptavidin-coated MμBs by washing twice with 1× PBS buffer, and then the

MμBs were mixed with biotinylated DNA at a molar ratio of 1:10^6. After reaction at 25 ± 2 °C for 1.0 h, the resulting DNA-modified MμBs were washed with 1× PBS buffer three times to remove unbound DNA.

Electrochemistry. All electrochemical measurements were performed using a CHI 650C potentiostat from CH Instruments (Austin, TX). A glassy carbon working electrode (GCE, 1.0 mm diameter), Ag/AgCl reference electrode, and Pt wire counter electrode were used for testing the DNA assay in a conventional electrochemical cell (Figure S3). For the oSlip-DNA device, all three electrodes were 2.0 mm in diameter and fabricated by stencil printing. The reference electrode was, therefore, a carbon quasi-reference electrode (CQRE), which holds a surprisingly stable potential for the duration of oSlip-DNA assays.

■ RESULTS AND DISCUSSION

Operation of the oSlip-DNA. In this section we explain the operation of the oSlip-DNA, including the one-step sample incubation procedure and anodic stripping voltammetry (ASV) detection method.

The three-strand DNA sandwich, which links together the AgNP labels and MμB solid supports, was carried out in a vial (i.e., off chip). Specifically, 50.0 μL of the HBV DNA target, present at different concentrations in 1× PBS buffer, was mixed with 10.0 μL of a 700 fM solution of the MμBs functionalized with the capture DNA and 10.0 μL of a 210.0 pM solution of AgNPs modified with the label DNA. After vortexing for 30.0 min, the mixture was washed twice using a magnet to retain the MμB-bound DNA sandwich. The DNA sandwich was then resuspended in 1× PBS buffer.

The assay begins by injecting the DNA sandwich into the inlet of the oSlip-DNA (Scheme 1a). The bottom of the main

Scheme 1

channel is rendered hydrophilic (the green hemichannel shown at the bottom of Scheme 1c),[44] so the MμBs will flow through the hollow channel due to capillary pressure. A small rare-earth magnet is positioned just above the working electrode and held in place by a plastic holder (Figure S2). Therefore, as the DNA sandwich moves down the channel, the MμBs are captured directly at the working electrode. This is an important preconcentration step that is, in part, responsible for the low LOD that characterizes the oSlip-DNA.

The channel and the sink at the end of the channel become saturated with solution within 15 s and flow stops. This results

in upward flow of the solution toward the outlet, and this in turn leads to resolution of the predispensed erioglaucine dye and the appearance of a blue color at the outlet of the oSlip-DNA. The appearance of the blue indicator means that flow has stopped and that the user should move the slip layer (the third layer) into its functional position (Scheme 1b). This results in 3.7 nmol of the oxidant (KMnO$_4$), which was predispensed onto a paper tab attached to the slip layer, being carried into the region of the channel directly below the working electrode. The solid KMnO$_4$ resolvates and diffuses through the ~180 μm thickness of the quiescent solution in the hollow channel within 20 s. This results in rapid oxidation of the AgNP labels by MnO$_4^-$ to yield soluble Ag$^+$.

The final step in the assay is to electrodeposit the free Ag$^+$ onto the working electrode, and then quantify the amount of zerovalent Ag by ASV. Because Ag$^+$ is confined within the narrow channel, the majority of it can be deposited onto the working electrode within 200 s. Each AgNP contains ~250,000 Ag atoms, and so this is the second source of chemical amplification that leads to low picomolar LODs. The entire analysis takes <5 min.
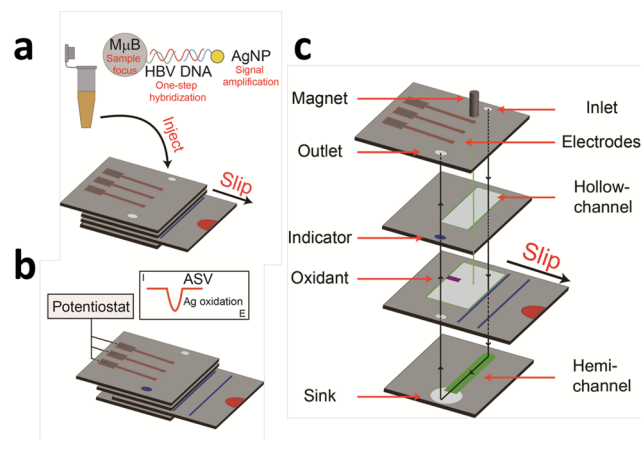
Characterization of DNA-Modified AgNPs and MμBs. It is not possible to directly measure the average number of oligonucleotides per AgNP using UV−vis spectroscopy, because the large AgNP plasmon peak at 400 nm overlaps the much smaller DNA absorbance at 260 nm (which is typically used for quantitation). However, using a very similar synthetic method, Liu and co-workers used fluorescently labeled DNA to estimate that there are ~220 DNA strands per 20 nm AgNP.[51]

Although it is difficult to know the average number of DNA molecules per AgNP, we have abundant circumstantial evidence for its presence. For example, the stability of the AgNPs is enhanced after DNA modification. This is demonstrated by the UV−vis spectra of AgNPs before and after modification with DNA (Figure S4). Before DNA modification, the AgNPs (diluted in DI H$_2$O) exhibit a large absorption peak at 400 nm, which is characteristic of the plasmon of individual AgNPs.[52,53] After washing the AgNPs and dispersing in 1× PBS buffer, however, the 400 nm absorption peak disappears, indicating agglomeration and precipitation.[54] In contrast, after the AgNPs are modified with DNA, the 400 nm plasmon peak is still evident after washing and dispersing in the same buffer. This enhanced stability in the high-salt buffer is a consequence of the stabilizing influence of the DNA shell.[55]

Additional evidence for the DNA shell comes from nanoparticle tracking analysis. Specifically, the zeta potential of the AgNPs decreases from −19.69 mV to −40.19 mV after modification with DNA. The negative zeta potential before DNA modification is probably due to the citrate capping reagent used during the initial synthesis of the AgNPs. The transmission electron micrographs in Figure S5 show that the size of AgNPs does not change during DNA modification, but the dispersion of particles is better due to DNA−DNA repulsion between particles. These results are consistent with the zeta potential measurements and the enhanced stability in salt solution, and together they strongly suggest the presence of DNA on the AgNPs.

It is easier to determine the amount of DNA on the 2.8 μm diameter MμBs than on the AgNPs. Specifically, we used UV−vis spectroscopy to determine the difference in DNA concentration in the supernatant before and after reaction with streptavidin coated MμBs, which corresponds to the

amount of DNA strands present on MμBs. The results show that there are $4.1 \pm 0.7 \times 10^5$ DNA strands per MμB.

DNA Sandwich Assay in a Conventional Electrochemical Cell. To benchmark the performance of the oSlip-DNA, the HBV DNA sandwich assay was carried out using a conventional electrochemical cell first. These experiments also provided us with an opportunity to optimize some parameters that could be transferred to the operation of the paper device.

Experiments in the conventional electrochemical cell were carried out as follows. Different concentrations of a 100.0 μL solution of the HBV DNA sandwich (see legend, Figure 1a),
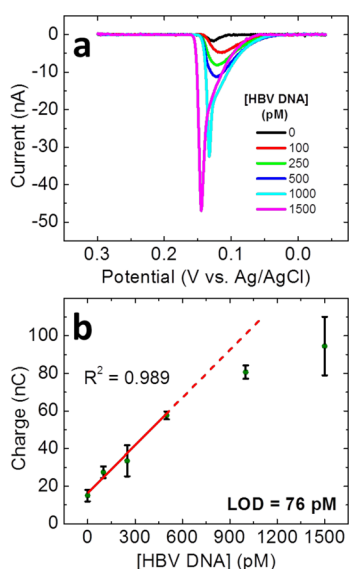

Figure 1. (a) ASVs obtained for the HBV DNA sandwich assay in a conventional electrochemical cell. Different concentrations of the HBV DNA target were mixed with 100 fM MμBs and 30.0 pM AgNPs in 1× PBS buffer for 30.0 min to form the DNA sandwich. Next, the DNA sandwich was added to a 1× PBS solution containing 41.6 μM KMnO$_4$. The ASVs of this solution were obtained by holding the potential of the working electrode at −0.30 V (vs Ag/AgCl) for 200 s and then scanning from −0.06 to 0.30 V at 10 mV/s. The data shown here has been baseline corrected. (b) Plot of charge under the ASVs shown in (a) as a function of the concentration of the HBV DNA target. The red line represents the best linear fit of the experimental data. The error bars reflect the standard deviations for replicate measurements carried out in three independently fabricated devices.

synthesized as described earlier, were added to a conventional electrochemical cell. Next, 1× PBS buffer (supporting electrolyte) and MnO$_4^-$ (oxidant, 41.6 μM final concentration)[4] were added to yield a total volume of 250.0 μL. After 20 s, which is sufficient time for MnO$_4^-$ to completely oxidize the AgNPs, three electrodes were inserted into the cell. Finally, the potential of the carbon working electrode was set to 0.30 V for 200 s, to electrodeposit Ag, and then ASV was initiated by scanning from −0.06 to 0.30 V at 10 mV/s. As shown in Figure 1a, Ag oxidation occurs at ~0.13 V.

The areas under the voltammograms in Figure 1a were integrated to determine the charge corresponding to Ag electrodeposited on the working electrode, and the resulting dose−response curve is plotted in Figure 1b. The plot is linear between target DNA concentrations ranging from 0 to 500 pM, but at higher concentrations the total charge collected is lower than predicted by the red line. This is probably due to the high-dose Hook effect, which is common in this type of one-step

sandwich assay.[56] The nonzero intercept in the plot is a consequence of nonspecific absorption of AgNPs on the MμBs. The LOD of the HBV DNA assay is 76 pM (i.e., 4.5×10^{10} DNA copies per mL), which is comparable to HBV DNA levels in the serum of patients before seroconversion.[57] This LOD is defined as three times the standard deviation of the blank signal, divided by the slope of dose−response curve in Figure 1b. Note that a control experiment was carried out using a target consisting of all T base single-stranded DNA (dT$_{30}$). The result (Figure S6) indicates a 4-fold higher signal for the correct target compared to dT$_{30}$. The signal for dT$_{30}$ is 2-fold higher than for the control experiment (no target present, Figure 1a).

After demonstrating the functionality of the sandwich assay, we turned our attention to optimizing three important experimental parameters to ensure the lowest possible LOD and efficient use of reagents. All of these experiments were carried out in the conventional electrochemical cell using the just-described procedure. First, the time required for DNA sandwich hybridization was studied. As shown in Figure 2a, the one-step sandwich reaction reached ~80% of its maximum signal at 30.0 min and plateaued thereafter, which is consistent with DNA binding kinetics under similar conditions.[58] Accordingly, 30.0 min was chosen as the optimal DNA hybridization time. Second, the effect of the MμB concentration on the Ag oxidation signal was tested while maintaining a 30.0 min DNA sandwich incubation time. The results in Figure 2b show that a MμB concentration of 100 fM is sufficient to capture most of the HBV DNA target strands. Beyond this point, no signal enhancement is observed. Third, the effect of the concentration of DNA-modified AgNPs was examined using a 30.0 min incubation time and 100 fM MμB concentration. Figure 2c shows that the signal increases with increasing AgNP concentration, but no limiting value is achieved. The reason for this behavior goes back to the Hook effect. That is, there is an excess of capture DNA strands (on the MμBs) but limited label strands (on the AgNPs), and therefore target DNA can only form a half-sandwich by binding to available capture strands. The higher the concentration of AgNPs (modified with label strands), the higher the chance of forming a complete sandwich and hence higher charge is observed. This argues for the use of higher AgNP concentrations, but to minimize nonspecific absorption of the AgNPs onto the MμBs, and to minimize cost, a AgNP concentration of 30.0 pM was chosen for the oSlip-DNA experiments.

DNA Sandwich Assay in the oSlip-DNA. Using the optimized parameters discussed in the previous section, we carried out a series of HBV DNA sandwich assays in the oSlip-DNA paper device. As for the experiments performed in the conventional electrochemical cell, 50.0 μL of the presynthesized DNA sandwich was injected into an oSlip-DNA device. As we have shown previously,[4] the magnet (Scheme 1c) concentrates the MμB-conjugated DNA sandwich on the surface of the working electrode. After ~12 s, flow stops due to saturation of the paper sink, which is indicated by the appearance of the blue dye at the outlet. At this point the slip layer is pulled to expose the AgNPs to the oxidant for 20 s. Finally, electrochemical detection is initiated by electrodepositing Ag$^+$ at −0.30 V for 200 s and then carrying out ASV from −0.30 to 0.30 V at 10 mV/s (in a preliminary report of the oSlip, we showed that these are the optimal values).[4]

The ASVs resulting from the foregoing procedure are shown in Figure 3a. Compared to the results obtained in the
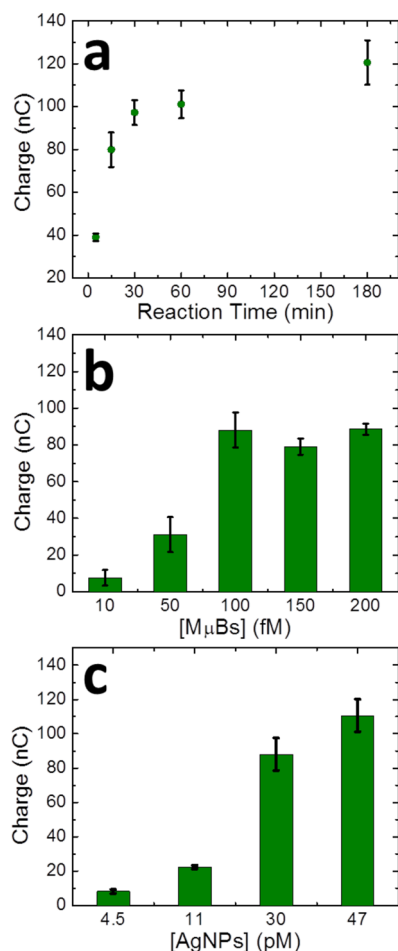
Figure 2. Optimization of reaction time and reagent concentrations. All experiments were performed in 1× PBS buffer and the concentration of the HBV DNA target used was 1.0 nM. Electrochemical measurements were carried out as in Figure 1. (a) Plot of charge under the ASV peaks as a function of reaction time. The HBV DNA target was mixed with 200 fM MμBs and 47.0 pM AgNPs for the indicated times. (b) Plot of charge under the ASV peaks as a function of MμB concentration. The HBV DNA target was mixed with 47.0 pM AgNPs and the indicated concentrations of MμBs for 30.0 min. (c) Plot of charge under the ASV peaks as a function of AgNP concentration. The HBV DNA target was mixed with 100 fM MμBs and the indicated concentrations of AgNPs for 30.0 min.

Figure 3. Results obtained using oSlip-DNA devices. (a) ASVs obtained for the HBV DNA sandwich assay. The indicated concentrations of the HBV DNA target were mixed with 100 fM MμBs and 30.0 pM AgNPs in 1× PBS buffer for 30.0 min. The electrochemical data were obtained by electrodepositing Ag at a potential of −0.30 V for 200 s and then scanning the potential from −0.30 to 0.30 V at 10 mV/s. The data shown here has been baseline corrected. (b) Plot of charge under the ASVs shown in part a as a function of the concentration of the HBV DNA target. The red line represents the best linear fit of the experimental data. The error bars reflect the standard deviations for replicate measurements carried out in three independently fabricated devices.

conditional electrochemical cell (Figure 1), there are two significant differences here. First, the potential range on the horizontal axis is different. This is because the oSlip uses a CQRE, which has a different potential than the Ag/AgCl reference electrode used to obtain the data in Figure 1a. Second, there is more variation in the Ag oxidation peak position in Figure 3a than in Figure 1a. This is also a consequence of the different reference electrodes used in the two experiments. Specifically, each ASV shown in Figure 3a was obtained using an independently fabricated oSlip, and there is some device-to-device variation in the potentials of the CQREs. This is not too big of a problem because it is still easy to integrate the peaks due to the absence of other electrochemical processes in this potential range.

Another important difference between the ASV results obtained in the conventional electrochemical cell (Figure 1a) and the oSlip-DNA (Figure 3a) is that the current is ∼25 times higher in the paper device even though the experimental
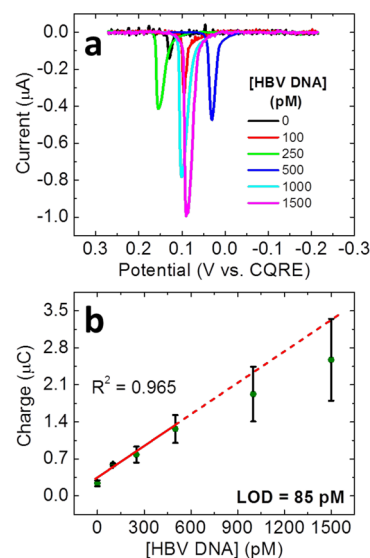
conditions are the same. We ascribe this difference primarily to the presence of the magnet above the working electrode (not present in the conventional electrochemical cell) and the concomitant accumulation of the MμB-bound AgNP labels. Additionally, there is an advantage to carrying out the Ag electrodeposition step in the oSlip due to its thinness and corresponding geometric confinement of Ag⁺ near the working electrode.[4,59] These factors represents the second level of amplification in the oSlip-DNA, the first being the 250 000-fold amplification of the sandwich due to oxidation of the AgNP labels. Note that in a preliminary report,[4] we showed that ∼84% of the MμBs introduced into the inlet of the oSlip-DNA are captured by the magnetic field in the vicinity of the working electrode.

Figure 3b is a plot of the charge under the ASV peaks in Figure 3a as a function of the concentration of HBV DNA. It exhibits a trend similar to that observed in the conventional electrochemical cell. That is, the ASV signal changes linearly with the HBV DNA concentrations ranging from 0 to 500 pM and presents a slight Hook effect at concentrations higher than 1.0 nM. As mentioned above, the charges under the ASV peaks are ∼25 times larger than that in the conventional electrochemical cell. However, the effect of AgNP nonspecific absorption on the MμBs also leads to a higher signal when no target is present. The LOD for the HBV DNA in the oSlip-DNA is 85 pM, about the same as in the conventional electrochemical cell (76 pM).

■ SUMMARY AND CONCLUSIONS

In conclusion, we have demonstrated the functionality of the oSlip-DNA for detection of HBV DNA using a one-step

sandwich assay. The *o*Slip-DNA is user-friendly, capable of handling assays that employ M*μ*Bs, and its two-stage amplification makes it possible to detect picomolar levels of the HBV DNA target. The dynamic range and linear range are 0−1.5 nM and 0−500 pM, respectively, with a LOD of 85 pM. Each sensor costs < $0.36 U.S. dollars to fabricate at the lab scale, and the assay is fast (<5 min) and robust compared to enzymatic amplification methods, making it a candidate for POC applications.

Still, there are some problems with the approach we described here. First, the DNA sandwich must be prepared ex situ, which for POC applications is not desirable. Accordingly, we are currently studying the feasibility of predispensing the M*μ*Bs functionalized with the capture sequences and the DNA-functionalized AgNP labels in the inlet of the device. This introduces a new set of problems, including reagent resolution, controlling the timing of the hybridization step, and issues related to nonspecific adsorption. We are also interested in more realistic matrixes (here we focused exclusively on buffer) and of course that introduces yet another set of challenges. Finally, the detection limit of the *o*Slip DNA for HBV is too high for direct assays. This means that some kind of nucleic acid preamplification, such as PCR, would be required for this particular HBV application. Note that it is not usual to couple off-chip PCR with PAD detection.[60] The results of our efforts to address these challenges will be reported in due course.

■ ASSOCIATED CONTENT

Ⓢ Supporting Information

The Supporting Information is available free of charge on the ACS Publications website at DOI: 10.1021/acs.anal-chem.5b02210.

> Design of the *o*Slip-DNA, photographs of the *o*Slip-DNA, photographs of the conventional electrochemical cell, UV−vis spectra of the AgNPs, transmission electron micrographs and size-distribution histograms for the AgNPs, and control experiment for the HBV DNA sandwich assay (PDF)

■ AUTHOR INFORMATION

Corresponding Author
*E-mail: crooks@cm.utexas.edu. Phone: 512-475-8674.
Notes
The authors declare no competing financial interest.

■ ACKNOWLEDGMENTS

■ REFERENCES

(1) Liu, H.; Crooks, R. M. *J. Am. Chem. Soc.* **2011**, *133*, 17564−17566.

(2) Du, W. B.; Li, L.; Nichols, K. P.; Ismagilov, R. F. *Lab Chip* **2009**, *9*, 2286−2292.

(3) Liu, H.; Li, X.; Crooks, R. M. *Anal. Chem.* **2013**, *85*, 4263−4267.

(4) Scida, K.; Cunningham, J. C.; Renault, C.; Richards, I.; Crooks, R. M. *Anal. Chem.* **2014**, *86*, 6501−6507.

(5) Dequaire, M.; Degrand, C.; Limoges, B. *Anal. Chem.* **2000**, *72*, 5521−5528.

(6) Renault, C.; Li, X.; Fosdick, S. E.; Crooks, R. M. *Anal. Chem.* **2013**, *85*, 7976−7979.

(7) Li, L.; Ismagilov, R. F. *Annu. Rev. Biophys.* **2010**, *39*, 139−158.

(8) Cao, Y. W. C.; Jin, R. C.; Mirkin, C. A. *Science* **2002**, *297*, 1536−1540.

(9) Rehermann, B.; Nascimbeni, M. *Nat. Rev. Immunol.* **2005**, *5*, 215−229.

(10) Bottcher, B.; Wynne, S. A.; Crowther, R. A. *Nature* **1997**, *386*, 88−91.

(11) Beasley, R. P.; Lin, C.-C.; Hwang, L.-Y.; Chien, C.-S. *Lancet* **1981**, *318*, 1129−1133.

(12) Brechot, C.; Scotto, J.; Charnay, P.; Hadchouel, M.; Degos, F.; Trepo, C.; Tiollais, P. *Lancet* **1981**, *318*, 765−768.

(13) Gupta, B. P.; Jayasuryan, N.; Jameel, S. *J. Clin. Microbiol.* **1992**, *30*, 1913−1916.

(14) Hadziyannis, S. J.; Lieberman, H. M.; Karvountzis, G. G.; Shafritz, D. A. *Hepatology* **1983**, *3*, 656−662.

(15) Ulrich, P. P.; Bhat, R. A.; Seto, B.; Mack, D.; Sninsky, J.; Vyas, G. N. *J. Infect. Dis.* **1989**, *160*, 37−43.

(16) Caliendo, A. M.; Valsamakis, A.; Bremer, J. W.; Ferreira-Gonzalez, A.; Granger, S.; Sabatini, L.; Tsongalis, G. J.; Wang, Y. F. W.; Yen-Lieberman, B.; Young, S. *J. Clin. Microbiol.* **2011**, *49*, 2854−2858.

(17) Li, M.; Cushing, S. K.; Liang, H.; Suri, S.; Ma, D.; Wu, N. *Anal. Chem.* **2013**, *85*, 2072−2078.

(18) Lu, X.; Dong, X.; Zhang, K.; Han, X.; Fang, X.; Zhang, Y. *Analyst* **2013**, *138*, 642−650.

(19) Bastian, L. A.; Nanda, K.; Hasselblad, V.; Simel, D. L. *Arch. Fam. Med.* **1998**, *7*, 465−469.

(20) Posthuma-Trumpie, G. A.; Korf, J.; van Amerongen, A. *Anal. Bioanal. Chem.* **2009**, *393*, 569−582.

(21) Martinez, A. W.; Phillips, S. T.; Butte, M. J.; Whitesides, G. M. *Angew. Chem., Int. Ed.* **2007**, *46*, 1318−1320.

(22) Martinez, A. W.; Phillips, S. T.; Whitesides, G. M. *Proc. Natl. Acad. Sci. U. S. A.* **2008**, *105*, 19606−19611.

(23) Martinez, A. W.; Phillips, S. T.; Whitesides, G. M.; Carrilho, E. *Anal. Chem.* **2010**, *82*, 3−10.

(24) Carrilho, E.; Phillips, S. T.; Vella, S. J.; Martinez, A. W.; Whitesides, G. M. *Anal. Chem.* **2009**, *81*, 5990−5998.

(25) Carrilho, E.; Martinez, A. W.; Whitesides, G. M. *Anal. Chem.* **2009**, *81*, 7091−7095.

(26) Fu, E.; Ramsey, S. A.; Kauffman, P.; Lutz, B.; Yager, P. *Microfluid. Nanofluid.* **2011**, *10*, 29−35.

(27) Ballerini, D. R.; Li, X.; Shen, W. *Microfluid. Nanofluid.* **2012**, *13*, 769−787.

(28) Hu, J.; Wang, S.; Wang, L.; Li, F.; Pingguan-Murphy, B.; Lu, T. J.; Xu, F. *Biosens. Bioelectron.* **2014**, *54*, 585−597.

(29) Cate, D. M.; Dungchai, W.; Cunningham, J. C.; Volckens, J.; Henry, C. S. *Lab Chip* **2013**, *13*, 2397−2404.

(30) Zhao, W.; Ali, M. M.; Aguirre, S. D.; Brook, M. A.; Li, Y. *Anal. Chem.* **2008**, *80*, 8431−8437.

(31) Dungchai, W.; Chailapakul, O.; Henry, C. S. *Anal. Chem.* **2009**, *81*, 5821−5826.

(32) Nie, Z. H.; Nijhuis, C. A.; Gong, J. L.; Chen, X.; Kumachev, A.; Martinez, A. W.; Narovlyansky, M.; Whitesides, G. M. *Lab Chip* **2010**, *10*, 477−483.

(33) Cunningham, J. C.; Brenes, N. J.; Crooks, R. M. *Anal. Chem.* **2014**, *86*, 6166−6170.

(34) Ellerbee, A. K.; Phillips, S. T.; Siegel, A. C.; Mirica, K. A.; Martinez, A. W.; Striehl, P.; Jain, N.; Prentiss, M.; Whitesides, G. M. *Anal. Chem.* **2009**, *81*, 8447−8452.

(35) Li, B.; Zhang, W.; Chen, L.; Lin, B. *Electrophoresis* **2013**, *34*, 2162−2168.

(36) Lee, C. H.; Hankus, M. E.; Tian, L.; Pellegrino, P. M.; Singamaneni, S. *Anal. Chem.* **2011**, *83*, 8953−8958.

(37) Scida, K.; Li, B. L.; Ellington, A. D.; Crooks, R. M. *Anal. Chem.* **2013**, *85*, 9713−9720.

(38) Luo, L.; Li, X.; Crooks, R. M. *Anal. Chem.* **2014**, *86*, 12390−12397.

(39) Delaney, J. L.; Hogan, C. F.; Tian, J.; Shen, W. *Anal. Chem.* **2011**, *83*, 1300−1306.

(40) Zhang, X.; Li, J.; Chen, C.; Lou, B.; Zhang, L.; Wang, E. *Chem. Commun.* **2013**, *49*, 3866−3868.

(41) Ho, J.; Tan, M. K.; Go, D. B.; Yeo, L. Y.; Friend, J. R.; Chang, H.-C. *Anal. Chem.* **2011**, *83*, 3260−3266.

(42) Maxwell, E. J.; Mazzeo, A. D.; Whitesides, G. M. *MRS Bull.* **2013**, *38*, 309−314.

(43) Liu, B.; Du, D.; Hua, X.; Yu, X. Y.; Lin, Y. *Electroanalysis* **2014**, *26*, 1214−1223.

(44) Renault, C.; Koehne, J.; Ricco, A. J.; Crooks, R. M. *Langmuir* **2014**, *30*, 7030−7036.

(45) Renault, C.; Anderson, M. J.; Crooks, R. M. *J. Am. Chem. Soc.* **2014**, *136*, 4616−4623.

(46) Fu, E.; Lutz, B.; Kauffman, P.; Yager, P. *Lab Chip* **2010**, *10*, 918−920.

(47) Li, X.; Zwanenburg, P.; Liu, X. *Lab Chip* **2013**, *13*, 2609−2614.

(48) Lutz, B. R.; Trinh, P.; Ball, C.; Fu, E.; Yager, P. *Lab Chip* **2011**, *11*, 4274−4278.

(49) Apilux, A.; Ukita, Y.; Chikae, M.; Chailapakul, O.; Takamura, Y. *Lab Chip* **2013**, *13*, 126−135.

(50) Zhang, X.; Servos, M. R.; Liu, J. *J. Am. Chem. Soc.* **2012**, *134*, 7266−7269.

(51) Zhang, X.; Servos, M. R.; Liu, J. W. *Chem. Commun.* **2012**, *48*, 10114−10116.

(52) Zou, S.; Janel, N.; Schatz, G. C. *J. Chem. Phys.* **2004**, *120*, 10871−10875.

(53) Lu, Y.; Liu, G. L.; Lee, L. P. *Nano Lett.* **2005**, *5*, 5−9.

(54) Chaloupka, K.; Malam, Y.; Seifalian, A. M. *Trends Biotechnol.* **2010**, *28*, 580−588.

(55) Cao, Y.; Jin, R.; Mirkin, C. A. *J. Am. Chem. Soc.* **2001**, *123*, 7961−7962.

(56) Rodbard, D.; Feldman, Y.; Jaffe, M.; Miles, L. *Immunochemistry* **1978**, *15*, 77−82.

(57) Chen, C. J.; Yang, H. I.; Iloeje, U. H. *Hepatology* **2009**, *49*, S72−S84.

(58) Drummond, T. G.; Hill, M. G.; Barton, J. K. *Nat. Biotechnol.* **2003**, *21*, 1192−1199.

(59) Bard, A. J.; Faulkner, L. R. *Electrochemical Methods: Fundamentals and Applications*, Vol. 2; Wiley: New York, 1980.

(60) Kim, Y. T.; Jung, J. H.; Choi, Y. K.; Seo, T. S. *Biosens. Bioelectron.* **2014**, *61*, 485−490.